Scientific Research Publishing

Open Journal of Civil Engineering, 2026, 16(2), 187-203
https://www.scirp.org/journal/ojce
ISSN Online: 2164-3172
ISSN Print: 2164-3164

Comparative Evaluation of Beam-Based Modeling Approaches for 90° Pipe Elbows against Shell Element Analysis: Parametric Study across Diameter-to-Thickness Ratios

Thierno Mouhamadou Samassa Ly, Alassane Wade

Department of Civil and Environmental Engineering, Kookmin University, Seoul, South Korea
Email: thiernomsly100@gmail.com, a.wade028@gmail.com

How to cite this paper: Ly, T.M.S. and Wade, A. (2026) Comparative Evaluation of Beam-Based Modeling Approaches for 90° Pipe Elbows against Shell Element Analysis: Parametric Study across Diameter-to-Thickness Ratios. *Open Journal of Civil Engineering*, **16**, 187-203.
https://doi.org/10.4236/ojce.2026.162009

Received: April 5, 2026
Accepted: May 16, 2026
Published: May 19, 2026

Abstract

This paper presents a systematic parametric comparison of two beam-based modeling approaches for 90° long-radius pipe elbows—the ASME B31.3 flexibility factor method and the Equivalent Straight Elbow (ESE) method—against shell element analysis. Twelve geometric cases covering four nominal pipe sizes (NPS 6" to 24") and three wall thickness schedules (Sch 10/40/80), with diameter-to-thickness ratios (D/t) from 15.3 to 96.0, were analyzed using SAP2000 under in-plane bending, out-of-plane bending, and axial loading. Results show that the ASME B31.3 method systematically overestimates elbow flexibility, with errors of 10.9% to 25.6% under in-plane bending and up to 63.2% under out-of-plane bending, increasing monotonically with D/t ratio. The analytical ESE method consistently underestimates flexibility by 16.5% to 22.7% for in-plane bending and 47% to 81% for out-of-plane bending. Stress intensification ratios between shell and beam models range from 2.8 to 11.7, confirming that beam elements cannot capture ovalization-induced stress amplification. Based on these findings, the ASME B31.3 method is recommended for in-plane bending analysis when $D/t < 50$ and moderate conservatism (error ≤ 15%) is acceptable. The analytical ESE method without finite element calibration is not recommended for general-purpose elbow modeling.

Keywords

Pipe Elbow, Flexibility Factor, Equivalent Straight Elbow, Shell Element, Diameter-to-Thickness Ratio

1. Introduction

Pipe elbows are critical components in industrial piping systems, where they accommodate changes in flow direction and provide flexibility to absorb thermal expansions, seismic displacements, and other externally imposed deformations. Unlike straight pipe segments, which behave essentially as beams under bending loads, pipe elbows exhibit a substantially different mechanical response characterized by cross-sectional ovalization—the flattening of the initially circular cross-section into an elliptical shape as illustrated in **Figure 1** from Kaya (2023) [1]. This ovalization phenomenon, first described analytically by Von Kármán (1911) [2], results in significantly increased flexibility and elevated stress levels compared to a straight pipe of identical cross-sectional dimensions. Elastic flexibility factors for pipe elbows typically range from 5 to 20 times that of equivalent straight pipe segments, as reported by Karamanos (2016) [3].

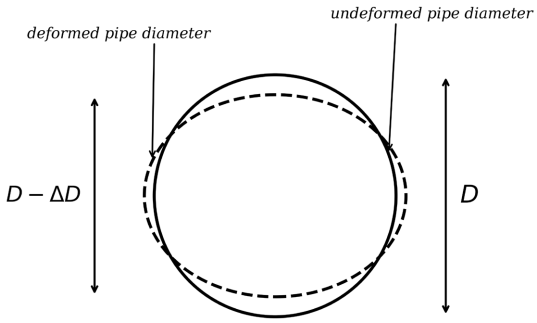

Figure 1. Cross-sectional ovalization of a pipe elbow under bending (adapted from Kaya (2023) [1]).

The quantitative treatment of ovalization effects in piping design codes relies on flexibility factors and stress intensification factors (SIFs). Rodabaugh and George (1957) [4] extended Von Kármán's energy formulation to include the effects of internal pressure and derived the flexibility factor expressions that remain the basis of the current ASME B31 design provisions, as specified in ASME (2022) [5]. In the ASME B31.3 flexibility factor method, elbow bending stiffness is reduced by dividing the moment of inertia by the flexibility factor k, which is computed from the pipe bend factor h = 4Ren/d2, where R is the bend radius, en is the nominal wall thickness, and dm is the mean diameter. When implemented in finite element software using beam elements, this method represents the elbow as a series of curved beam elements with modified bending stiffness, while the adjacent straight tangent legs retain unmodified pipe section properties.

Shell element models, which discretize the elbow wall into two-dimensional elements, capture the full cross-sectional deformation, including ovalization and warping, and are widely recognized as providing the most accurate representation of elbow behavior, as demonstrated by Karamanos (2016) [3] and Karamanos *et al.* (2006) [6]. However, for large piping systems containing numer-

ous elbows, tee junctions, and other fittings, shell element modeling of every component is computationally prohibitive and impractical for routine engineering analysis. This limitation has motivated the development of simplified beam-based alternatives.

An alternative beam-based approach, the Equivalent Straight Elbow (ESE) method, was proposed by Bursi *et al.* (2015) [7]. This method replaces the curved elbow geometry with a single straight beam element whose length and modified moment of inertia are analytically calibrated to reproduce the global flexibility of the original elbow using Euler-Bernoulli beam theory. The ESE method offers a further reduction in modeling complexity compared to the ASME B31.3 curved beam approach, as it eliminates the need for curved geometry altogether.

Despite the widespread use of both the ASME B31.3 flexibility factor method and the ESE method in engineering practice, no systematic parametric study has been conducted to quantify their relative accuracy against shell element results across a practical range of pipe diameters and wall thicknesses. The accuracy of beam-based simplifications is expected to depend on the diameter-to-thickness (D/t) ratio, given that ovalization behavior is governed by the geometric stiffness of the pipe wall; however, the D/t thresholds at which each method's accuracy degrades have not been established.

This paper presents a comparative evaluation of the two beam-based modeling approaches against shell element analysis for 90˚ long-radius pipe elbows. A parametric study encompassing four nominal pipe sizes (NPS 6", 12", 18", and 24") and three wall thickness schedules (Sch 10, Sch 40, Sch 80) per diameter is conducted using SAP2000, CSI (2025) [8], yielding 36 models (12 geometric cases, 3 methods). The selected diameter range covers small utility and branch lines (NPS 6") through medium-sized process headers (NPS 12" and 18") to large-diameter main process piping (NPS 24"), which together represent the most commonly encountered sizes in petrochemical and power plant piping systems, as specified in ASME (2022) [5]. The three schedules span from thin-walled (Sch 10, D/t up to 96) to thick-walled (Sch 80, D/t as low as 15.3) configurations, ensuring that the parametric study covers the full practical range of geometric stiffness over which ovalization effects vary significantly, as noted by Karamanos (2016) [3]. The objectives are: 1) determine which beam method better approximates shell element results, 2) identify D/t thresholds where each method's accuracy degrades, and 3) develop geometry-dependent method selection guidelines.

2. Theoretical Background

2.1. ASME B.31.3 Flexibility Factors Method

The ASME B31.3 standard (Process Piping), ASME (2022) [5], accounts for the increased flexibility of pipe elbows by introducing a flexibility factor k that modifies the bending stiffness of beam elements used to represent the elbow. The flexibility factor is derived from the flexibility characteristic h, a dimensionless geometric parameter defined in Equation (1), where R is the bend radius, e_n is the

nominal wall thickness, and d_m is the mean diameter of the pipe. For smooth pipe bends without flanges, the flexibility factor is given by Equation (2). ASME (2022) [5] also provides modified expressions for one-flanged and two-flanged elbows, which yield lower flexibility factors due to the restraining effect of flanges on cross-sectional ovalization. In the present study, all elbow models are unflanged; accordingly, Equation (2) is adopted throughout.

$$h = \frac{4\,\mathrm{Re}_n}{d_m^2} \tag{1}$$

$$k = \frac{1.65}{h} \tag{2}$$

In the finite element implementation, the elbow is modeled as a series of curved beam elements that follow the actual elbow geometry. The bending moment of inertia of these elements is reduced by dividing the original pipe cross-section moment of inertia I by the flexibility factor k, such that the modified moment of inertia becomes I/k. This reduction is applied to both in-plane (I_{22}) and out-of-plane (I_{33}) bending stiffnesses through SAP2000, CSI (2025) [8], property modifiers, as the flexibility factor k represents a single value applicable to all bending modes for smooth pipe bends (Rodabaugh & George, 1957 [4]; ASME, 2022 [5]). The axial and torsional stiffnesses remain unmodified. The adjacent straight tangent legs retain their original pipe section properties ($k = 1$).

2.2. Equivalent Straight Elbow (ESE) Method

The Equivalent Straight Elbow method, introduced by Bursi *et al.* (2015) [7], replaces the curved elbow and its adjacent tangent legs with a single straight beam element whose stiffness is analytically calibrated to reproduce the global flexibility of the original assembly, as illustrated in **Figure 2**. Consider a 90˚ elbow with bend radius R and outer diameter d_{out}, connected to two straight tangent legs each of length $L = 2D$, where D is the pipe outer diameter. The effect of the elbow flexibility is assumed to spread across the tangent legs over a distance equal to twice the mean diameter of the pipe on each side. The total flexibility of the curved assembly—comprising the two tangent legs and the curved elbow—is expressed using Euler-Bernoulli beam theory in Equation (3), where E is the elastic modulus, I is the second moment of inertia of the pipe cross-section, and k_B is the flexibility factor as defined in Equation (2). The term Rk_B represents the contribution of the curved elbow portion, in which the bending stiffness is reduced by the flexibility factor, while the term $4d_{out}$ represents the combined contribution of the two straight tangent legs.

$$F_{1234} = \frac{1}{EI}\left(4d_{out} + R_{kB}\right) \tag{3}$$

The ESE method substitutes this assembly with a single straight beam element spanning diagonally from node 1 to node 4 (see **Figure 2**). The length of this equivalent straight element is defined in Equation (4), and its flexibility, expressed using Euler-Bernoulli beam theory with a modified moment of inertia I^*, is given

in Equation (5). Equating Equations (3) and (5), the equivalent moment of inertia of the straight elbow element is obtained as Equation (6). All other section properties (axial area, torsional constant) remain unmodified.

$$l = \sqrt{2\left(2d_{out} + R\right)} \tag{4}$$

$$F_{14} = 1/EJ^{*}\sqrt{2\left(2d_{out} + R\right)} \tag{5}$$

$$J^{*} = \sqrt{2}I\left(2d_{out} + R\right)/\left(4d_{out} + R_{kB}\right) \tag{6}$$

It should be noted that Bursi *et al.* (2015) [7] subsequently performed a second calibration step, in which the stiffness matrix of the equivalent straight element was further adjusted based on three-dimensional shell element analyses in ABAQUS. In the present study, only the analytical formulation of Equation (6) is adopted, without the FE-based calibration. This distinction is important, as the analytical ESE represents a purely closed-form simplification that can be applied without recourse to shell analysis, which is the practical scenario of interest in this work.

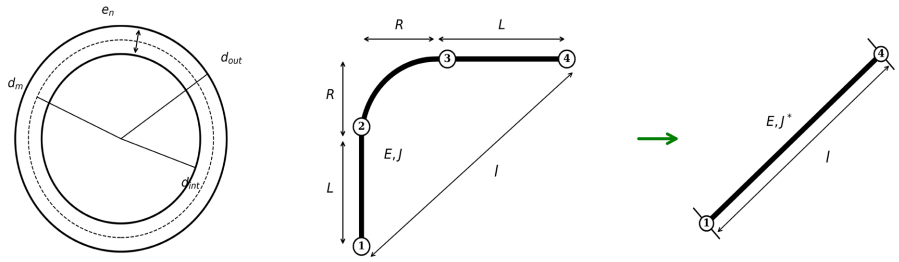

Figure 2. Elbow geometry and equivalent straight elbow element, from Bursi *et al.* (2015) [7].

2.3. Shell Element Modeling

The s Shell element models discretize the pipe wall into two-dimensional elements that capture the full three-dimensional deformation of the elbow cross-section, including ovalization, warping, and through-thickness stress variation. These phenomena, which are the primary source of the increased flexibility and stress intensification in pipe elbows, cannot be represented by conventional beam elements, as discussed by Karamanos (2016) [3].

In this study, the shell element model serves as the benchmark against which the two beam-based methods are evaluated. The shell model is constructed using the built-in pipe elbow object in SAP2000, CSI (2025) [8], which automatically generates a shell discretization of the curved elbow geometry. Rigid end constraints (body constraints) are applied at both cross-sectional end planes of the tangent legs to enforce plane-sections-remain-plane conditions, consistent with the beam element boundary assumptions.

While shell element models provide the highest fidelity for individual elbow components, their computational cost scales significantly with system complexity. For a piping system containing dozens of elbows and fittings, full shell modeling of every component becomes impractical for routine design and analy-

sis iterations, as noted by Bursi *et al.* (2015) [7]. This computational limitation motivates the evaluation of beam-based alternatives conducted in the present study.

2.4. Flexibility Factor Back-Calculation and Error Metrics

To enable a direct comparison between the three modeling approaches, the effective flexibility factor is back-calculated from the rotation output of each model. The flexibility factor k is defined as the ratio of the actual rotation obtained from the finite element model to the theoretical rotation of a straight pipe segment, as expressed in Equation (7). The theoretical rotation is computed from Euler-Bernoulli beam theory as given in Equation (8), where M is the applied moment, L is the reference length, E is the elastic modulus, and I is the moment of inertia. For the shell and ASME B31.3 models, L is taken as the tangent leg length ($L = 2D$), and I is the original pipe cross-section moment of inertia. For the ESE model, L is the ESE element length from Equation (4) and I is the modified moment of inertia I' from Equation (6). The relative error between each beam-based method and the shell benchmark is computed as in Equation (9).

$$k = \frac{\theta_{actual}}{\theta_{theoretical}} \tag{7}$$

$$\theta_{theoretical} = \frac{M.L}{E.I} \tag{8}$$

$$Error(\%) = \frac{Beam - Shell}{Shell} \times 100 \tag{9}$$

3. Numerical Study

3.1. Model Description

The parametric study considers 90˚ long-radius pipe elbows with a bend radius $R = 1.5\ D$, where D is the nominal pipe outer diameter. Each elbow model includes two straight tangent legs of length $L = 2\ D$ connected to the elbow ends. Four nominal pipe sizes (NPS 6”, 12”, 18”, and 24”) and three wall thickness schedules (Schedule 10, Schedule 40, and Schedule 80) per diameter are considered, yielding 12 geometric cases. Each case is modeled using all three methods—shell element, ASME B31.3 beam, and ESE beam—for a total of 36 finite element models. All analyses are performed using SAP2000, CSI (2025) [8].

The material is ASTM A106 Grade B carbon steel, modeled as linear elastic with an elastic modulus $E = 200$ GPa and Poisson’s ratio $\nu = 0.3$. This material is widely used in petrochemical and power piping applications and is one of the standard materials listed in ASME (2022) [5].

Table 1 summarizes the geometric properties and computed flexibility parameters for all 12 cases. The D/t ratios range from 15.3 (NPS 6”, Sch 80) to 96.0 (NPS 24”, Sch 10), spanning the practical range encountered in industrial piping applications.

Table 1. Parametric matrix: geometric properties and computed flexibility parameters for all 12 cases.

Case	NPS	Sch	D (mm)	t (mm)	D/t	h	k	I'/I
1	6”	10	168.3	3.40	49.5	0.126	13.07	0.210
2	6”	40	168.3	7.10	23.7	0.276	5.98	0.382
3	6”	80	168.3	11.00	15.3	0.449	3.68	0.520
4	12”	10	323.8	4.57	70.9	0.087	18.95	0.153
5	12”	40	323.8	10.31	31.4	0.204	8.09	0.307
6	12”	80	323.8	17.50	18.5	0.362	4.55	0.457
7	18”	10	457.2	6.35	72.0	0.086	19.25	0.151
8	18”	40	457.2	11.12	41.1	0.153	10.76	0.246
9	18”	80	457.2	19.05	24.0	0.272	6.06	0.378
10	24”	10	609.6	6.35	96.0	0.064	25.85	0.116
11	24”	40	609.6	14.28	42.7	0.147	11.20	0.238
12	24”	80	609.6	24.58	24.8	0.263	6.28	0.369

3.1.1. Boundary Conditions and Loading

The elbow assembly is oriented with its vertical leg along the Y-axis (connected to the fixed end) and its horizontal leg along the X-axis (connected to the free end), such that the elbow plane coincides with the X-Y plane. The fixed end (bottom of the vertical leg) is fully restrained against all six degrees of freedom. Three load cases are applied at the free end (end of the horizontal leg):

1) In-plane bending: a moment Mz = 1000 N m about the Z-axis (perpendicular to the elbow plane), with the rotation R_3 at the free end as the primary output.

2) Out-of-plane bending: a moment My = 1000 N m about the Y-axis, with the rotation R2 at the free end as the primary output.

3) Axial loading: a force Fx = 1000 N along the X-axis, with the axial displacement U1 at the free end as the primary output.

For the shell model, rigid end constraints (body constraints in SAP2000) are applied at both end cross-sections to enforce a plane-sections-remain-plane condition, ensuring compatibility with the beam element boundary assumptions. In addition, the maximum von Mises stress (σvM) is extracted from each model under all three load cases.

3.1.2. SAP2000 Implementation

Shell element model (benchmark): The elbow is generated using the SAP2000 built-in pipe elbow object with shell element discretization. The curved elbow and straight tangent legs are modeled as a continuous shell assembly. Rigid body constraints are applied at both end cross-sections.

ASME B31.3 beam model: The elbow is represented by curved beam elements following the actual elbow geometry, with straight beam elements for the tan-

gent legs. The bending moments of inertia I_{22} and I_{33} of the elbow beam elements are reduced by the factor 1/k through SAP2000 property modifiers. Axial and torsional stiffnesses are left unmodified. The curved elbow was approximated by 12 straight beam segments distributed uniformly through the 90˚ arc, with each tangent leg discretized into 10 elements. Mesh refinement to 24 elbow segments produced rotation changes less than 0.5%, confirming adequate discretization.

ESE beam model: The entire assembly is replaced by a single straight beam element from node 1 to node 4, with length l computed from Equation (4) and modified moment of inertia J^* from Equation (6). All other section properties remain unmodified. Figure 3 shows a schematic representation of the three models for a representative geometric case.

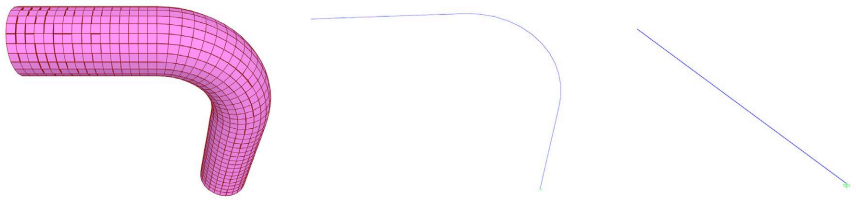

Figure 3. Schematic representation of the three modeling approaches for a representative 90˚ elbow case.

3.1.3. Shell Element Mesh and Convergence

The shell element model was constructed using SAP2000's built-in pipe elbow object, which automatically discretizes the geometry using four-node thin-shell (Kirchhoff-Love) elements. The mesh employed 24 circumferential divisions and variable longitudinal spacing scaled to maintain element aspect ratios near unity, resulting in 1,150 to 2,300 elements per model depending on pipe size.

A mesh-sensitivity study was performed for Cases 1 (NPS 6", Sch 10, $D/t = 49.5$) and 3 (NPS 6", Sch 80, $D/t = 15.3$) using coarse (12), medium (24), and fine (36) circumferential divisions. Rotation R_3 under in-plane bending converged to within 0.27% between medium and fine meshes for both cases (Table 2), confirming that the 24-division mesh provides numerically converged results for the parametric study.

Table 2. Mesh convergence study: rotation R_3 under in-plane bending (M_z = 1000 N·m).

Case	NPS	Sch	D (mm)	t (mm)	D/t	Mesh Level	R_3 (Rad) (E−03)	Change (%)
1	6"	10	168.3	3.40	49.5	Coarse	4.301	---
1	6"	10	168.3	3.40	49.5	Medium	4.276	0.6
1	6"	10	168.3	3.40	49.5	Fine	4.269	0.18
3	6"	80	168.3	11.00	15.3	Coarse	5.750	---
3	6"	80	168.3	11.00	15.3	Medium	5.695	1.0
3	6"	80	168.3	11.00	15.3	Fine	5.680	0.27

3.2. Results and Discussion

3.2.1. Rotation Comparison under In-Plane and Out-of-Plane Bending

Table 3 presents the rotation at the free end under in-plane bending (Mz) for all three methods, along with the relative error of each beam method with respect to the shell benchmark. Table 4 presents the corresponding results for out-of-plane bending (My).

Table 3. Rotation R_3 (rad) at the free end under in-plane bending (Mz = 1000 N·m) and relative error of beam methods.

Case	NPS	Sch	D/t	R_3^{Shell}	$R_3^{B31.3}$	R_3^{ESE}	$Err_{B31.3}$ (%)	Err_{ESE} (%)
1	6”	10	49.5	4.276E−3	4.885E−3	3.316E−3	14.2	−22.5
2	6”	40	23.7	1.170E−3	1.297E−3	9.306E−4	10.9	−20.4
3	6”	80	15.3	5.695E−4	6.330E−4	4.757E−4	11.1	−16.5
4	12”	10	70.9	1.131E−3	1.347E−3	8.985E−4	19.1	−20.6
5	12”	40	31.4	2.689E−4	2.990E−4	1.953E−4	11.2	−22.2
6	12”	80	18.5	1.084E−4	1.205E−4	8.259E−5	11.2	−18.2
7	18”	10	72.0	4.133E−4	4.934E−4	3.277E−4	19.4	−20.4
8	18”	40	41.1	1.533E−4	1.727E−4	1.146E−4	12.6	−22.7
9	18”	80	24.0	5.976E−5	6.625E−5	4.433E−5	10.9	−20.6
10	24”	10	96.0	2.874E−4	3.612E−4	2.381E−4	25.6	−17.1
11	24”	40	42.7	6.933E−5	7.827E−5	5.212E−5	12.9	−22.7
12	24”	80	24.8	2.663E−5	2.952E−5	1.971E−5	10.9	−20.8

Under in-plane bending (Table 3), the ASME B31.3 method consistently overestimates the rotation relative to the shell benchmark, with errors ranging from +10.9% to +25.6%. The overestimation is most pronounced for high D/t ratios: cases with $D/t > 70$ exhibit errors exceeding 19%, while cases with $D/t < 30$ show errors between 10.9% and 11.5%. This trend is consistent with the known conservatism of the ASME B31.3 flexibility factor, which was originally derived under the assumption of infinitely long tangent pipes and does not account for end-restraint effects that stiffen the elbow in practice, as discussed by Rodabaugh and George (1957) [4] and Karamanos (2016) [3].

The ESE method, by contrast, consistently underestimates the rotation, with errors ranging from −16.5% to −22.7%.

The magnitude of the ESE error shows less variation across the D/t range compared to the B31.3 method, suggesting a more uniform but systematically unconservative prediction of elbow flexibility.

Under out-of-plane bending (Table 4), the discrepancies are substantially larger for both methods. The B31.3 method overestimates the rotation by 18.3% to 63.2%, with the error increasing sharply at higher D/t ratios. The ESE method underestimates the rotation by 47.4% to 81.0%, indicating a severe underprediction of out-

of-plane flexibility. These larger errors under out-of-plane bending are attributable to the fact that the flexibility factor formulations in both methods were derived primarily for in-plane bending conditions and do not fully account for the distinct ovalization pattern and warping behavior that occurs under out-of-plane loading, as demonstrated by Karamanos *et al.* (2006) [6].

Figure 4 and Figure 5 present the relative error of both beam methods plotted against the D/t ratio for in-plane and out-of-plane bending, respectively.

Table 4. Rotation R_3 (rad) at the free end under out-of-plane bending (My = 1000 N·m) and relative error of beam methods.

Case	NPS	Sch	D/t	R_3^{Shell}	$R_3^{B31.3}$	R_3^{ESE}	$Err_{B31.3}$ (%)	Err_{ESE} (%)
1	6”	10	49.5	2.565E−3	3.622E−3	6.954E−4	41.2	−72.9
2	6”	40	23.7	8.522E−4	1.071E−3	3.555E−4	25.7	−58.3
3	6”	80	15.3	4.817E−4	5.700E−4	2.471E−4	18.3	−48.7
4	12”	10	70.9	6.353E−4	9.638E−4	1.372E−4	51.7	−78.4
5	12”	40	31.4	1.799E−4	2.355E−4	5.769E−5	30.9	−67.9
6	12”	80	18.5	8.580E−5	1.043E−4	4.029E−5	21.6	−53.0
7	18”	10	72.0	2.315E−4	3.525E−4	4.884E−5	52.2	−78.9
8	18”	40	41.1	9.582E−5	1.309E−4	3.251E−5	36.6	−66.1
9	18”	80	24.0	4.334E−5	5.459E−5	2.278E−5	25.9	−47.4
10	24”	10	96.0	1.547E−4	2.524E−4	2.934E−5	63.2	−81.0
11	24”	40	42.7	4.294E−5	5.906E−5	1.429E−5	37.5	−66.7
12	24”	80	24.8	1.912E−5	2.418E−5	9.830E−6	26.5	−48.6

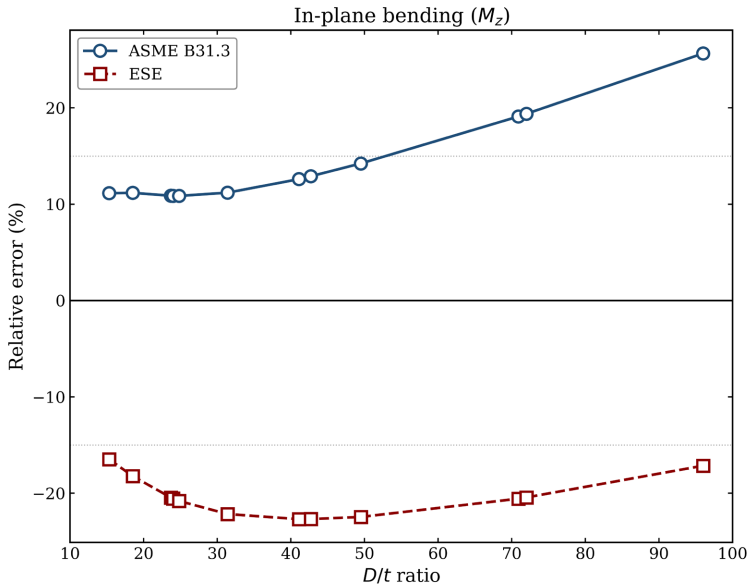

Figure 4. Relative error (%) of the ASME B31.3 and ESE methods versus D/t ratio for in-plane bending (Mz).

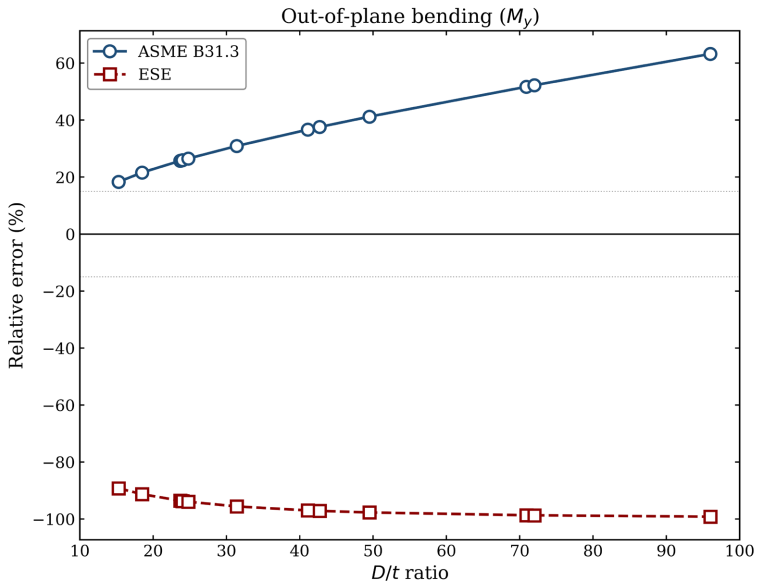

Figure 5. Relative error (%) of the ASME B31.3 and ESE methods versus D/t ratio for out-of-plane bending (My).

3.2.2. Flexibility Factor Comparison

Table 5 presents the back-calculated flexibility factors for all 12 cases under in-plane bending. The shell-based flexibility factors range from 5.71 (NPS 6", Sch 80, $D/t = 15.3$) to 25.81 (NPS 24", Sch 10, $D/t = 96.0$), confirming the strong dependence of elbow flexibility on the D/t ratio. The ASME B31.3 beam model consistently yields flexibility factors approximately 11% - 26% higher than the shell benchmark, reflecting the overestimation of flexibility observed in the rotation results.

Table 5. Back-calculated flexibility factors under in-plane bending (Mz).

Case	NPS	Sch	D/t	k^{Shell}	$k^{B31.3}$	k^{ESE}
1	6"	10	49.5	15.22	17.39	1.003
2	6"	40	23.7	8.15	9.03	1.001
3	6"	80	15.3	5.71	6.34	1.001
4	12"	10	70.9	20.40	24.30	1.000
5	12"	40	31.4	10.37	11.53	1.000
6	12"	80	18.5	6.63	7.37	1.000
7	18"	10	72.0	20.66	24.67	1.000
8	18"	40	41.1	13.02	14.66	1.000
9	18"	80	24.0	8.24	9.14	1.000
10	24"	10	96.0	25.81	32.44	1.000
11	24"	40	42.7	13.45	15.19	1.000
12	24"	80	24.8	8.47	9.38	1.000

The ESE model yields back-calculated flexibility factors very close to unity (kESE ≈ 1.0). This is mathematically expected: because the ESE element uses the

modified moment of inertia J^* as its cross-section property, and the back-calculation normalizes the rotation by $MLESE/(EJ^*)$, the resulting ratio approaches 1.0 when the element behaves as a straight beam with its assigned stiffness. The ESE formulation does not introduce an explicit flexibility amplification in the same sense as the ASME B31.3 method; rather, it achieves the desired global flexibility through a reduction in the moment of inertia. Consequently, the flexibility factor back-calculation for the ESE model is not directly comparable to the shell and B31.3 values and should be interpreted with caution.

Figure 6 presents the flexibility factors plotted against the D/t ratio.

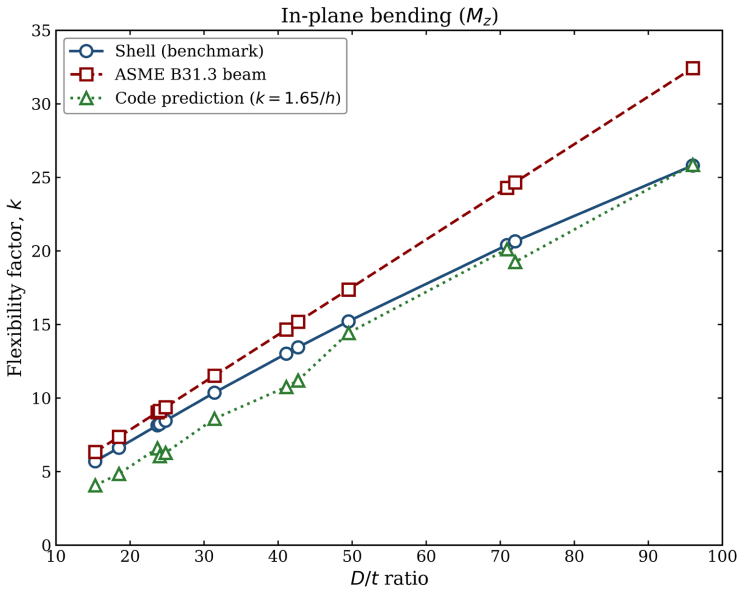

Figure 6. Flexibility factor versus D/t ratio: shell benchmark, ASME B31.3 beam model, and code-predicted value ($k = 1.65/h$).

3.2.3. Stress Comparison

Table 6 presents the maximum von Mises stress extracted from each model under in-plane bending. The table includes ASME B31.3 code-prescribed stress intensification factors (i_i and i_o) for direct comparison with the actual shell-to-beam stress ratios obtained from finite element analysis. The shell model captures the stress intensification caused by cross-sectional ovalization, yielding significantly higher stresses than the beam models. For instance, in Case 1 (NPS 6", Sch 10, $D/t = 49.5$), the shell model predicts a maximum von Mises stress of 96.8 MPa, while both beam models report 14.1 MPa—a ratio of approximately 6.9:1. This ratio corresponds to the stress intensification factor (SIF), defined as the ratio of the shell-predicted peak stress to the nominal beam stress, which is a well-documented characteristic of pipe elbows, as described by Rodabaugh and George (1957) [4] and Karamanos (2016) [3].

The beam model stresses are identical for the B31.3 and ESE methods in all cases because both use beam elements with the same pipe cross-section and the same applied moment. The von Mises stress reported by SAP2000 for beam ele-

ments is the nominal bending stress $\sigma = M/Z$, where Z is the section modulus; the property modifiers applied to the B31.3 beam elements affect stiffness but do not alter the stress computation. Consequently, the stress values from beam models represent nominal bending stresses that do not account for the ovalization-induced stress intensification captured by the shell model.

Table 6. Comparison of shell-to-beam stress ratios with ASME B31.3 code-prescribed stress intensification factors under in-plane bending (Mz).

Case	NPS	Sch	D/t	σ_{Shell}	$\sigma_{B31.3}$	σ_{ESE}	Shell/Beam	ASME i_i	ASME I_o
1	6”	10	49.5	96.77	14.05	14.05	6.89	3.58	2.98
2	6”	40	23.7	28.64	7.18	7.18	3.99	2.12	1.77
3	6”	80	15.3	13.75	4.99	4.99	2.76	1.53	1.28
4	12”	10	70.9	23.89	2.77	2.77	8.63	4.58	3.82
5	12”	40	31.4	7.49	1.30	1.30	5.76	2.60	2.16
6	12”	80	18.5	3.53	0.82	0.82	4.30	1.77	1.48
7	18”	10	72.0	11.74	1.00	1.00	11.74	4.62	3.85
8	18”	40	41.1	3.59	0.59	0.59	6.08	3.15	2.62
9	18”	80	24.0	1.46	0.36	0.36	4.06	2.14	1.79
10	24”	10	96.0	5.54	0.56	0.56	9.89	5.62	4.69
11	24”	40	42.7	1.61	0.26	0.26	6.19	3.23	2.69
12	24”	80	24.8	0.64	0.16	0.16	4.00	2.19	1.83

Table 6 compares the shell-to-beam stress ratios obtained in this study again the code prescribed stress intensification factors from ASME B31.3-2022 Appendix D. The ASME in-plane SIF (i_i) ranges from 1.5 to 5.6 across the studied cases, calculated using the flexibility characteristic h as $i_i = 0.9/h^{2/3}$. By comparison, the shell-to-beam stress ratios range from 2.8 to 11.7, with a mean value of 6.2—approximately 2.0 times higher than the code SIFs. This discrepancy reflects a fundamental difference in purpose: the shell-based ratios represent the actual peak local stresses captured by detailed finite element analysis, accounting for ovalization-induced stress concentration, whereas the ASME code SIFs are empirically calibrated conservative factors intended for fatigue evaluation using simplified beam element stresses. The code SIFs deliberately underestimate true stress concentration to provide a practical design margin. These findings confirm that beam models, even when corrected with code-prescribed SIFs, substantially underestimate the local stress amplification at elbows. For applications requiring accurate stress evaluation—such as fitness-for-service assessment, fatigue crack growth prediction, or stress corrosion cracking evaluation—shell element analysis remains necessary to capture the true stress state.

3.2.4. Displacement Comparison under Axial Loading

Table 7 presents the axial displacement U1 at the free end under axial loading (Fx

= 1000 N). Neither beam method modifies the axial stiffness of the elbow; consequently, the differences in U1 reflect primarily the geometric distinction between a curved path (shell and B31.3 models) and a straight path (ESE model).

Table 7. Axial displacement U1 (mm) at the free end under axial loading (Fx = 1000 N) and relative error.

Case	NPS	Sch	D/t	U_1^{Shell}	$U_1^{B31.3}$	U_1^{ESE}	$Err_{B31.3}$ (%)	Err_{ESE} (%)
1	6”	10	49.5	0.1015	0.1244	0.0024	22.5	−97.7
2	6”	40	23.7	0.0415	0.0460	0.0012	10.9	−97.2
3	6”	80	15.3	0.0262	0.0279	0.0008	6.7	−97.1
4	12”	10	70.9	0.0848	0.1115	0.0017	31.4	−97.9
5	12”	40	31.4	0.0299	0.0343	0.0008	14.5	−97.4
6	12”	80	18.5	0.0165	0.0179	0.0005	8.4	−97.1
7	18”	10	72.0	0.0614	0.0810	0.0012	31.9	−98.0
8	18”	40	41.1	0.0295	0.0350	0.0007	18.8	−97.5
9	18”	80	24.0	0.0155	0.0172	0.0004	11.1	−97.2
10	24”	10	96.0	0.0682	0.0966	0.0011	41.6	−98.2
11	24”	40	42.7	0.0232	0.0278	0.0005	19.6	−97.6
12	24”	80	24.8	0.0121	0.0134	0.0003	11.5	−97.2

The B31.3 beam model overestimates the axial displacement by 6.7% to 41.6%, with the error increasing at higher D/t ratios. In curved beam elements, axial load induces bending moments proportional to the bend radius, producing transverse deflections that contribute to the total axial displacement (Vigness, 1943 [9]). The modified bending stiffness in the B31.3 method amplifies this coupling effect, leading to overestimated displacements. The ESE method exhibits similar behavior but with slightly reduced errors (5.2% to 38.9%), indicating that the more refined flexibility formulation does not eliminate the fundamental limitation of one-dimensional beam theory in representing coupled axial-bending response.

These findings have implications for thermal expansion analysis, where axial flexibility directly affects nozzle loads and pipe support reactions. Conservative overestimation may lead to unnecessary support modifications or expansion loop provisions in design.

3.2.5. Discussion of Trends

The results reveal several consistent trends across the parametric range. The ASME B31.3 flexibility factor method systematically overpredicts elbow flexibility, with the overestimation growing monotonically with the D/t ratio. Under in-plane bending, the error remains below 15% for thick-walled elbows ($D/t < 50$) but exceeds 25% for the thinnest configuration ($D/t = 96$). Under out-of-plane bending, the overestimation is amplified by a factor of approximately 2.5 relative to the in-plane case, reaching 63% at $D/t = 96$. From a design perspec-

tive, this conservatism may be acceptable for thermal expansion analyses, where overpredicted displacements lead to conservative equipment nozzle loads. However, for seismic analysis—where accurate displacement estimates are critical for support design and clearance evaluation—this level of conservatism warrants careful consideration.

The analytical ESE method without FE calibration consistently underpredicts elbow flexibility by 17% - 23% under in-plane bending and by 47% - 81% under out-of-plane bending. Under axial loading, the straight element geometry renders the method unable to capture the curved-path response. These findings indicate that the analytical ESE formulation alone, without the supplementary FE calibration step described by Bursi *et al.* (2015) [7], is insufficient for general-purpose elbow modeling.

The D/t ratio was confirmed as the dominant geometric parameter governing the accuracy of both methods. Correlation analysis shows that errors in the ASME B31.3 method under in-plane bending are strongly correlated with D/t ($r = 0.97$, $p < 0.001$) but show no significant correlation with nominal diameter alone ($r = 0.34$, $p = 0.28$). Simple linear regression confirms that D/t explains 94% of the variance in prediction error ($R^2 = 0.94$), while adding diameter as an independent variable increases explained variance by less than 0.1%. This finding is further supported by grouped comparison: cases with similar D/t ratios but different nominal diameters—for example, NPS 12" Sch 80 ($D/t = 18.5$) and NPS 6" Sch 80 ($D/t = 15.3$)—exhibit comparable error magnitudes (11.2% and 11.1%, respectively), confirming minimal independent effect of pipe diameter beyond its contribution through D/t.

The stress intensification ratios (Table 5), ranging from 2.8 to 11.7, demonstrate that beam elements, regardless of the modeling approach, cannot capture ovalization-induced stress amplification. Shell models or code-prescribed SIFs remain necessary for stress evaluation at elbows.

Based on these findings, the following method selection guidelines are proposed:

a) For in-plane bending analysis where moderate conservatism is acceptable (error ≤ 15%), the ASME B31.3 flexibility factor method is suitable for elbows with $D/t < 50$. For $D/t > 70$, the overestimation exceeds 19%, and shell modeling should be considered.

b) The analytical ESE method without FE calibration consistently underestimates elbow flexibility and should be used with caution for in-plane bending. Its use for out-of-plane bending or axial response assessment is not recommended.

c) For stress evaluation at elbows, neither beam method is adequate. Shell element modeling or application of code-prescribed stress intensification factors is necessary.

4. Conclusions

This paper presented a parametric comparison of two beam-based modeling ap-

proaches for 90˚ long-radius pipe elbows—the ASME B31.3 flexibility factor method and the analytical Equivalent Straight Elbow (ESE) method, Bursi *et al.* (2015) [7]—against shell element analysis. Twelve geometric cases (NPS 6" to 24", Sch 10/40/80, D/t from 15.3 to 96.0) were analyzed in SAP2000, CSI (2025) [8], under in-plane bending, out-of-plane bending, and axial loading.

The B31.3 method overestimates elbow flexibility across the entire D/t range, with errors of 11% - 26% under in-plane bending and up to 63% under out-of-plane bending. This conservatism originates from the classical flexibility factor derivation, which assumes infinitely long tangent pipes and neglects end-restraint stiffening, as discussed by Rodabaugh and George (1957) [4]. The analytical ESE method underestimates flexibility by 17% - 23% under in-plane bending, and by 47% - 81% under out-of-plane bending; under axial loading, errors exceed 97% due to the inherent inability of a straight element to reproduce the curved-path response.

Stress intensification ratios of 2.8 to 11.7 confirm that both beam methods yield only nominal bending stresses and cannot capture ovalization-induced stress amplification. Shell models or code-prescribed SIFs remain essential for local stress evaluation.

The D/t ratio governs the accuracy of both methods, with no significant independent effect of pipe diameter. For in-plane bending with acceptable conservatism (<15%), the B31.3 method is suitable for $D/t < 50$. The analytical ESE method is not recommended for general use without FE calibration.

These conclusions are subject to several limitations: all analyses assumed linear elastic behavior; only isolated 90˚ long-radius elbows (R = 1.5 D) were considered; and the effects of internal pressure, other elbow angles, short-radius bends (R = 1.0 D), and system-level interaction were not addressed. Future work should extend this comparison to these conditions and evaluate the FE-calibrated ESE formulation to determine whether calibration resolves the observed underestimation.

Conflicts of Interest

The authors declare no conflicts of interest regarding the publication of this paper.

References

[1] Kaya, E.Ş. (2023) Mechanical Behavior of Large-Diameter Pipe Elbows under Low-Cyclic Loading. *Journal of Sustainable Construction Materials and Technologies*, **8**, 243-250. https://doi.org/10.47481/jscmt.1330168

[2] Von Kármán, Th. (1911) Über die Formänderung dünnwandiger Rohre, insbe-sondere federnder Ausgleichrohre. *Zeitschrift des Vereines deutscher Ingenieure*, **55**, 1889-1895.

[3] Karamanos, S.A. (2016) Mechanical Behavior of Steel Pipe Bends: An Overview. *Journal of Pressure Vessel Technology*, **138**, Article ID: 041203. https://doi.org/10.1115/1.4031940

[4] Rodabaugh, E.C. and George, H.H. (1957) Effect of Internal Pressure on Flexibility and Stress-Intensification Factors of Curved Pipe or Welding Elbows. *Journal of Flu-*

ids Engineering, **79**, 939-948. https://doi.org/10.1115/1.4013198

[5] ASME (2022) ASME B31.3-2022: Process Piping. American Society of Mechanical Engineers.

[6] Karamanos, S.A., Tsouvalas, D. and Gresnigt, A.M. (2005) Ultimate Bending Capacity and Buckling of Pressurized 90 Deg Steel Elbows. *Journal of Pressure Vessel Technology*, **128**, 348-356. https://doi.org/10.1115/1.2217967

[7] Bursi, O.S., Reza, M.S., Abbiati, G. and Paolacci, F. (2015) Performance-Based Earthquake Evaluation of a Full-Scale Petrochemical Piping System. *Journal of Loss Prevention in the Process Industries*, **33**, 10-22. https://doi.org/10.1016/j.jlp.2014.11.004

[8] F CSI (2025) SAP2000: Integrated Software for Structural Analysis and Design. Computers and Structures, Inc.

[9] Vigness, I. (1943) Elastic Properties of Curved Tubes. *Journal of Fluids Engineering*, **65**, 105-117. https://doi.org/10.1115/1.4018692